The Use of System Identification Methods to Evaluate the Effects of Slider-Disk Contacts and Disk Micro-Waviness on the Flying Height Modulations

Saurabh K. Deoras[1]
e-mail: sdeoras@talkelab.ucsd.edu

Frank E. Talke
e-mail: ftalke@ucsd.edu

Center for Magnetic Recording Research,
Department of Mechanical and Aerospace Engineering,
University of California, San Diego,
San Diego, CA 92093-0401

System identification methods have been used to study the response of a magnetic recording slider during contact with a scratch on the disk surface. In addition, the slider response was studied taking into account the effect of disk micro-waviness at various disk rotational speeds. The simulated slider response was compared with the measured slider dynamic behavior. Very good agreement was found between simulated and measured data. The flying height modulation of the slider, due to disk micro-waviness, was found to depend on disk velocity. [DOI: 10.1115/1.2162551]

Introduction

With the recent reduction in the flying height (FH) of magnetic recording sliders, the ratio of flying height modulation (FHM) to flying height has decreased further [1]. Zeng et al. have measured the flying height modulations using the read-back signal and have shown that a flying height jump during writing process can result in an unacceptable drive error and data loss [2]. Yim et al. have shown that the baseline instability of the read signal is linearly proportional to the amplitude of the disk surface waviness [3]. In addition, large flying height modulation can lead to intermittent slider-disk contacts especially for ultra low flying height sliders. Zeng et al. have measured repeatable and nonrepeatable flying height modulations and have found that the repeatable part of the flying height modulations attained a minimum at steady flying conditions [4]. They have also shown that disk waviness and roughness do not directly result in a strong air-bearing resonance. Thornton et al. have characterized flying height modulation for different frequency ranges [5] and have found that the flying height modulation of a sub-10 nm flying air-bearing slider in the low frequency range, i.e., between 10 and 100 kHz, was on the same order as the disk topography. Flying height modulation in the frequency range from 100 to 500 kHz is dominated by the response of the slider air-bearing. Disk waviness and roughness have strong effects on the slider take-off height [6]. Since ultra low flying sliders require very low take-off heights, smoother disk surfaces are required. Zhaoguo et al. have reported that lower substrate micro-waviness can result in the reduction of the minimum allowable bump height in the laser texture zone [7]. Thus, the reduction of flying height modulation is of increasing importance when the flying height is decreased to lower and lower values. Based on numerical simulation studies, Xu et al. have proposed that a slider exhibiting reduced flying height modulations from disk waviness should be designed without side pads or with side pads far away from the trailing edge [8].

In this paper we investigate the effect of disk micro-waviness on the dynamic response of a magnetic recording slider. Here, micro-waviness is defined as topography of the disk surface with wavelengths in the range from 4 to 900 μm. The following procedure is used: First the motion of the slider is measured using a laser Doppler vibrometer (LDV). Thereafter, the profile of the disk surface is characterized again using laser Doppler vibrometry. In all measurements precise triggering and signal averaging was used to improve measurement accuracy. Using the measured data, we employ parametric system identification methods to develop a model of the slider response. The model is then used to simulate the effect of disk micro-waviness on the slider dynamics. Excellent correlation between simulation results and experimental observations is found to occur. To study the effect of micro-waviness as a function of velocity, we have interpolated the measured disk profile. The results show that disk micro-waviness increases flying height modulation as a function of disk velocity. This indicates that the effect of disk micro-waviness must be evaluated at the disk velocity at which the particular head-disk interface is intended to be used.

Experimental Setup

A schematic of the experimental setup used in this work is shown in Fig. 1. The experimental apparatus consists of a variable speed motor, a spindle to clamp a 95 mm form factor disk and a high speed data acquisition system. The pico sliders used in the study have a nominal flying height of 8 nm at 5400 rpm (15.5 m/s). The head-gimbal assembly (HGA) is mounted on an actuator arm which is locked in a position corresponding to the middle diameter (MD) of the disk. The laser spot from the laser Doppler vibrometer (LDV) is focused on the gimbal which covers the back side of the slider, i.e., the laser cannot access the slider directly. The LDV has a bandwidth ranging from 10 kHz to 1.5 MHz. The disks used in our study were coated with 1.6 nm of Z-Dol lubricant. The centerline average roughness (R_a) of the disks, measured with an atomic force microscope (AFM), is 0.28 nm. A scratch on the disk in the radial direction is used as the source of excitation for the slider. The scratch, shown in Fig. 2, is made using a sharp needle. The dimensions of the scratch, measured with an optical profilometer (WYKO), are approximately 50 μm in width and 15 nm in height.

Using this experimental setup we obtained LDV velocity data of the slider response. More than 100 individual time signals, all cross-correlated at the slider-scratch impact, were averaged to reduce noise. The process of cross-correlated averaging of signals involves taking the time domain average of signals which are perfectly correlated with each other. After completing the mea-

[1]Address all correspondence to this author.

Contributed by the Tribology Division of ASME for publication in the JOURNAL OF TRIBOLOGY. Manuscript received February 25, 2004; final manuscript received October 2, 2005. Review conducted by Jeffrey Streator.

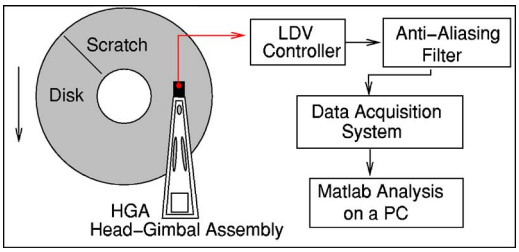

Fig. 1 Schematic of experimental setup

surement of the slider response, the slider was removed and LDV measurements of the disk surface were performed. Again, all signals were cross-correlated and averaged to reduce measurement noise.

Model of Slider Response

Figure 3 shows a typical experimental result for the velocity and power spectrum of the vibration signal at the center trailing (ct) edge of the slider after a scratch impact. We observe that the slider response is characteristic for a multiple degree of freedom

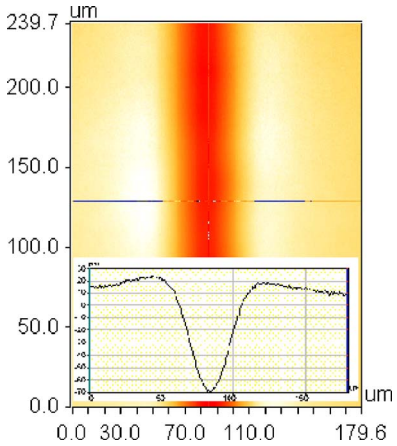

Fig. 2 Dimensions of the scratch as measured with an optical profilometer (WYKO)

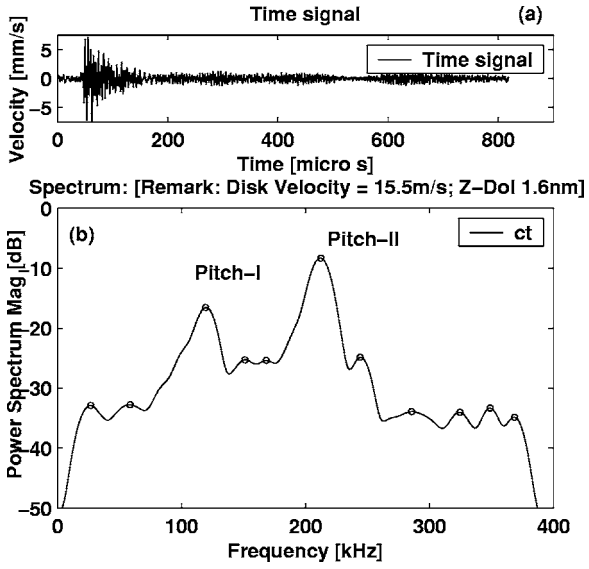

Fig. 3 Velocity and power spectrum of slider after scratch impact

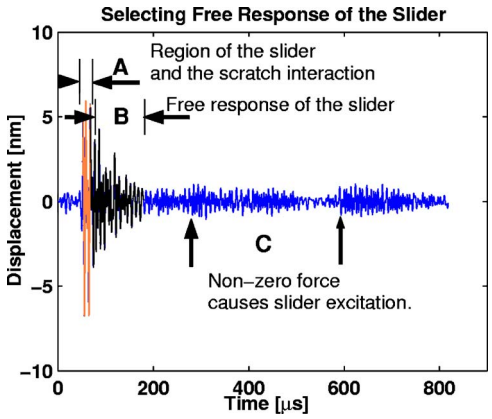

Fig. 4 Displacement signal: Various sections

system. In particular, two pitch modes are present, denoted by pitch-I and pitch-II, at frequencies 112 and 212 kHz, respectively. To develop a model of the slider response we use the theory of system identification. The slider air-bearing system is modeled with external forces as the input and the slider response as the output. The cross-correlated and averaged velocity signal is first integrated digitally to give the displacement signal in Fig. 4. This displacement signal can be divided into three distinct regions. The first region, denoted by "A," corresponds to the time interval when the impact between slider and the scratch occurs. This impact excites the slider vibrations. In the following region, region "B," the slider vibrations dampen out. This section is referred to as the "free-response" of the slider.

To develop a system identification model of the slider response we use the "free-response" region of the displacement signal as the output of the model. Figure 5 shows the block diagram of the modeling procedure. Input $u(t)$ is the force exerted on the slider due to the scratch impact and output $y(t)$ is the measured free response of the slider. The measured response $y(t)$ is the sum of the simulated response $Y(t)$ and the error component $v(t)$. We assume that the error signal $v(t)$ takes into account the measurement noise and the noise in the input signal. The input force on the slider caused by the scratch impact is an impulsive force. Since the magnitude of the force is not known, we use a normalized value to build the model, i.e., we assume a force of unit magnitude. The calculated output $Y(t)$ at any time t can be written as a linear combination of past input values $u(t)$ and output values $y(t)$ [9]. A vector containing input and output values ($\psi(t)$) and a vector containing coefficients (θ), for linear combination of $u(t)$ and $y(t)$, can be defined as follows [9]:

$$\psi(t) = [-y(t-1) \ \cdots \ -y(t-n) \ u(t-1) \ \cdots \ u(t-m)]^T \quad (1)$$

$$\theta = [a_1 \cdots a_n \ b_1 \cdots b_m]^T \quad (2)$$

The output $Y(t)$ can be written as a linear combination of input and output values:

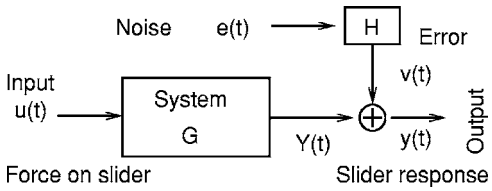

Fig. 5 Defining the system model

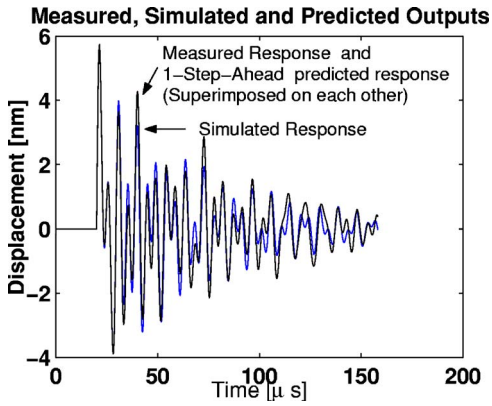

Fig. 6 Comparison of measured output, one-step-ahead prediction and simulation

$$Y(t|\theta) = \psi^T(t)\theta \tag{3}$$

If Z^N is a vector containing the input and output values over a time interval $1 \leqslant t \leqslant N$:

$$Z^N = \{u(1), y(1), \ldots, u(N), y(N)\}, \tag{4}$$

than the coefficients in θ can be determined using a least square approach by minimizing the error between the calculated value $Y(t)$ and the measured output $y(t)$ [9]:

$$\min_{\theta} V_N(\theta, Z^N) \tag{5}$$

where

$$V_N(\theta, Z^N) = \frac{1}{N}\sum_{t=1}^{N}(y(t) - Y(t|\theta))^2 = \frac{1}{N}\sum_{t=1}^{N}(y(t) - \psi^T(t)\theta)^2 \tag{6}$$

The values of θ for which the error $V_N(\theta, Z^N)$ is a minimum are denoted by $\hat{\theta}_N$ [9]:

$$\hat{\theta}_N = \left[\sum_{t=1}^{N}\psi(t)\psi^T(t)\right]^{-1}\sum_{t=1}^{N}\psi(t)y(t) \tag{7}$$

The number of input values (m) and output values (n) determine the order of the model. G and H are the system model and error model, respectively, which are transfer functions. Thus, for a given arbitrary input sequence $u^*(t)$, the simulated output $y^*(t)$ is given by the relation [9]:

$$y^*(t) = G(q)u^*(t) = \sum_{k=1}^{\infty} g(k)u^*(t-k) \tag{8}$$

The "one-step-ahead" prediction of the output at time t, from the known values of input $u(t)$ and the output $y(t-1)$, up to time $t-1$, is computed as follows:

$$y(t|t-1) = H^{-1}(q)G(q)u(t) + [1 - H^{-1}(q)]y(t) \tag{9}$$

The frequency response of the model can be determined using the system model G. It should be noted that the model developed in this way does not use modal properties of the mechanical system. The measured output $y(t)$ can then be written as:

$$y(t) = Y(t) + v(t) = G(q)u(t) + H(q)e(t) \tag{10}$$

where $e(t)$ is white Gaussian noise. Figure 6 shows three curves: Fig. 6(a) the measured free response of the slider, Fig. 6(b) the "one-step-ahead" predicted output, and Fig. 6(c) the simulated impulse response of the slider. We observe that the predicted and the simulated output results are in very close agreement with the measured data. In particular, as is shown in Fig. 6, there is no discernible difference between the measured velocity and the results from one-step-ahead prediction. The one-step-ahead prediction shows a correlation of 99%, while the simulated output shows a correlation of about 72% with the measured response. Thus, it is apparent that the system identification model describes the slider response very well. Figure 7 shows the Bode magnitude diagram of the model on a log-log scale. We observe that the model picks up three modes of vibrations of the slider, i.e., roll, pitch-I and pitch-II.

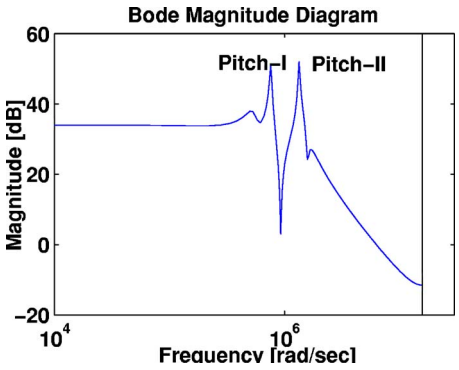

Fig. 7 Bode diagram of the model

Results and Discussion

Figure 8 shows the calculated impulse response of the slider air-bearing based on system identification. We observe that the amplitude of the simulated slider vibrations decay with time to zero. On the other hand, the measured vibrations, shown in Fig. 4, do not decay to zero. We conjecture that this discrepancy between the measured and calculated results is due to disk micro-waviness. Disk micro-waviness causes perturbations in the air-bearing force which excites the slider motion. Since the perturbations in the air-bearing force caused by disk micro-waviness are small for the roughness amplitude considered in this study, we hypothesize that air-bearing force perturbations are proportional to the time-varying amplitude of disk micro-waviness. To test this hypothesis we simulated the slider response by evaluating our model with force perturbations proportional to the amplitude of disk micro-waviness.

A typical amplitude distribution of disk micro-waviness is shown in Fig. 9 as a function of the reciprocal wavelength. The rate at which this micro-waviness is "seen" by the slider is a function of the disk velocity. In Fig. 10 the slider response is calculated at 3000 rpm (8.5 m/s) for the disk micro-waviness of Fig. 9, with the assumption that the perturbations in the air-bearing force due to disk micro-waviness are proportional to the time-varying amplitude of disk micro-waviness. We observe that the slider displacement decreases to nearly zero after 200 μs.

The simulation of the slider response in the presence of disk micro-waviness at 6000 rpm (17 m/s) is shown in Fig. 11. We

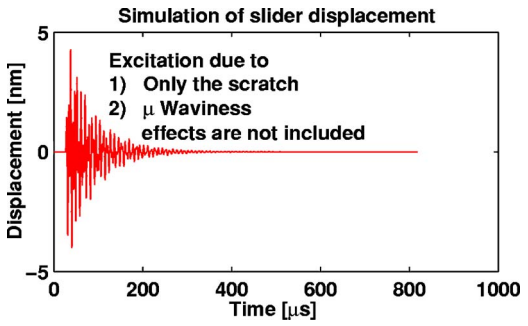

Fig. 8 Impulse response for the slider using the model

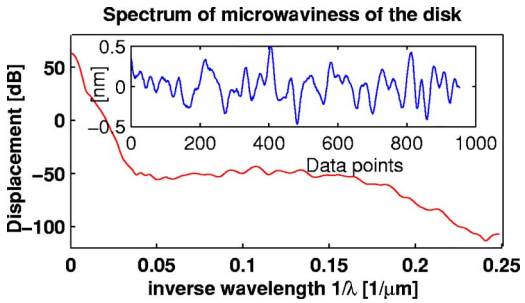

Fig. 9 Micro-waviness on the disk surface

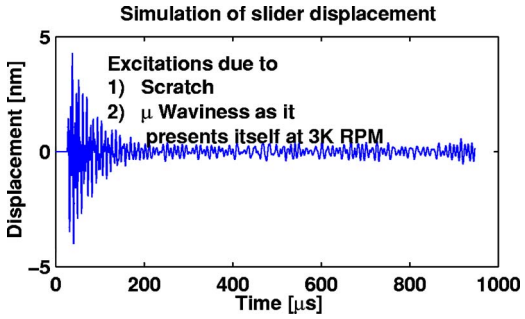

Fig. 10 Effect of disk micro-waviness at 3*k* rpm (8.5 m/s)

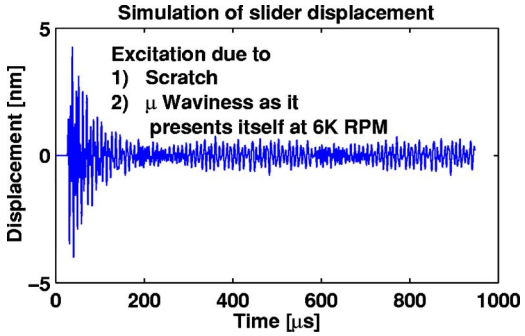

Fig. 11 Effect of disk micro-waviness at 6*k* rpm (17 m/s)

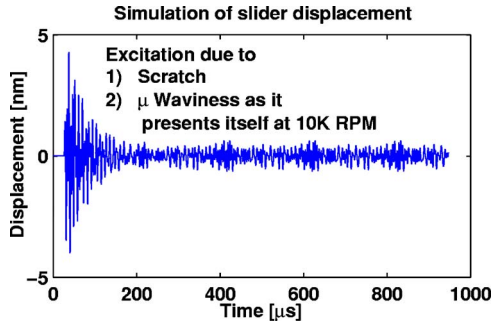

Fig. 12 Effect of disk micro-waviness at 10*k* rpm (28.5 m/s)

observe that the calculated slider displacement is different from that shown in Fig. 10. In particular, we note that the slider vibrations do not go to zero, but show amplitude modulations even after 200 μs. Comparing Fig. 11 with the experimental results of Fig. 4 we observe that the slider response after 200 μs is very similar in both cases. Thus, the hypothesis that the time-dependent air-bearing force due to the disk micro-waviness creates flying height modulations seems to be in excellent agreement with experimental measurements. In Fig. 12 the effect of disk micro-waviness on flying height modulation is shown for 10,000 rpm (28.5 m/s). At this velocity, flying height modulations are very small. Thus, the effects of disk micro-waviness on flying height modulations appears to be a strong function of velocity, being most critical for a velocity close to 6000 rpm (17 m/s).

Summary and Conclusion

System identification methods have been used to develop a model for the response of a slider after having contact with a scratch on the disk. We have evaluated the model using measured disk roughness profiles and have simulated the response of the slider air-bearing as a function of velocity. The key assumption made is that the perturbation of the time-varying air-bearing force is proportional to the magnitude of the disk micro-waviness. The results show that simulation and experimental observations are in excellent agreement with each other.

From our study we conclude:

(1) System identification methods can be used effectively to describe the flying height response of a slider as a function of different input conditions.
(2) Disk micro-waviness causes flying height modulation of the slider.
(3) The effect of disk micro-waviness on flying height modulation is a function of disk velocity. The effect of surface micro-waviness must therefore be determined at the velocity for which the slider interface is designed.

Acknowledgment

We would like to thank Yiao-Tee Hsia (Seagate) for helpful discussions in this study and Qing Zhao (Seagate) for providing disks and magnetic recording sliders for our experiments.

References

[1] Yao, W., Kuo, D., and Gui, J., 1999, "Effects of Disc Micro-Waviness in an Ultra-High Density Magnetic Recording System," *Proc. Symp. Interface Tech. Toward 100 Gb/in*^{2}, ASME, pp. 31–37.
[2] Zeng, Q. H., and Chen, M., 2003, "Flying Height Modulation Estimation From Pseudorandom Readback Signal in Disk Drives," IEEE Trans. Magn., **39**(5), pp. 2417–2419.
[3] Yim, P., Wang, P., Li, Z., Danen, T., Choa, S., and Lee, H. J., 1999, "The Role of Disk Surface Waviness on Baseline Instability of MR Head," IEEE Trans. Magn., **35**(2), pp. 758–763.
[4] Zeng, Q. H., Thorton, H., Bogy, D. B., and Bhatia, C. S., 2001, "Flyability and Flying Height Modulation Measurement of Sliders With Sub-10 nm Flying Heights," IEEE Trans. Magn., **37**(2), pp. 894–899.
[5] Thornton, B., Bogy, D. B., and Bhatia, C. S., 2002, "The Effects of Disk Morphology on Flying-Height Modulation: Experiment and Simulation," IEEE Trans. Magn., **38**(1) pp. 107–111.
[6] Gonzales, D., Nayak, V., Marchon, B., Payne, R., Crump, D., and Denning, P., 2001, "The Dynamic Coupling of the Slider to the Disk Surface and Its Relevance to Take-Off Height," IEEE Trans. Magn., **37**(4), pp. 1839–1841.
[7] Zhaoguo, J., Yang, M. M., Sullivan, M., Chao, J. L., and Russak, M., 1999, "Effect of Micro-Waviness and Design of Landing Zones With a Glide Avalanche Below 0.5μ'' for Conventional Pico Sliders," IEEE Trans. Magn., **35**(5), pp. 2370–2372.
[8] Xu, J., and Liu, B., 2003, "Flying Height Modulation and Femto Slider Design," IEEE Trans. Magn., **39**(5), pp. 2438–2440.
[9] Ljung, L., 1999, *System Identification: Theory for the User*, Prentice-Hall PTR, Englewood Cliffs, NJ.